Strain-Stress Formation and Deformation of Molded Materials by Drying-Induced Shrinkage

Yoshinori Itaya[1,*]

[1]Environmental and Renewable Energy Systems Division, Graduate School of Engineering, Gifu University, 1-1, Yanagido, Gifu, 501-1193, Japan

Abstract. Drying-induced strain-stress and deformation was modeled for molded materials such as ceramics and foods. The transient three-dimensional problem of strain-stress and heat and moisture transfer was solved simultaneously by the finite element method. The behaviors of internal strain-stress formation and deformation are compared among three modes of hot air heating, intermittent heating and internal heating for a ceramic slab. The concepts of the mass transfer potential and a linear viscoelasticity were introduced to consider the different sorption isotherm for layered foods consisting of two ingredients and creep phenomenon. The tensile and compressive stresses fluctuate and fall remarkably during lower heating period when the slab is heated intermittently. In the internal heating mode, drying proceeds fastest as well as stress formation is maintained at the lowest level in the three modes. This effectiveness of the internal heating is investigated experimentally by employing the microwave heating as well. The combination of different foods influences significantly not only the drying characteristic but also the internal strain-stress generation. The drying behavior could be analyzed with a high accuracy even if only heat and moisture transfer were solved without strain-stress analysis. This fact results in that heat and mass transfer and strain-stress are not always necessary to be analyzed simultaneously for saving the CPU time.

1Introduction

Drying-induced failures and deformation of molded materials are substantially undesirable problems for the quality control in the production process. If drying of molded materials is hastened, the surface does not only dry up immediately and the drying rate falls markedly maintaining a wet state in the inside, but also medium is subjected to strong internal stress and the product results in generation of failures in the worst case. In order to maintain the minimum stress formation during drying, the internal migration rate of moisture should be improved or an appropriate operation of the drying should be carried out so to reduce the gradient of the moisture content profile. Theoretical studies have been carried out for solving numerically the drying problems including shrinkage of clay in the past works [1-3]. However, there have been rather few researches from the viewpoint of failure and effective drying processes.

[*]Corresponding author: yitaya@gifu-u.ac.jp

The present author performed R&D on modeling of drying-induced strain-stress [4-6] and some parametric analyses of the strain-stress in the drying process are performed to investigate the influence of heating modes on the behaviors of drying-induced strain-stress and deformation as well as the drying characteristic [7]. The transient three-dimensional problem of strain-stress and heat and moisture transfer in a slab is solved simultaneously by the finite element method. The modes of convective, intermittent and internal heating are introduced by modeling them in the normalized parameters. The experiment is also carried out to examine the effect of drying characteristic by microwave heating which is one of the promising internal heating modes [8, 9].

Drying of foods is an important process for preservation preventing deterioration and maintaining nutrition for a long term. There are several foods consisting of multi-ingredients whose sorption isotherm of moisture is different. The most foods generate also drying-induced shrinkage that causes strain and stress. In order to produce high quality molded foods in a drying process, accurately appropriate controls are necessary not so to form failures and unacceptable irregular deformation. However, there has been only a little works on modeling to analytically predict such a complicated drying behavior except for some works [10-14] Those model should combine simultaneously the drying-induced strain-stress and moisture migration taking account for different sorption isotherm or concept of chemical potential [15] between wet multi-solids to carry out accurate analyses. This author has developed also a generally applicable computerized method for predicting three dimensional heat and moisture transfer with viscoelastic strain-stress in macroscopically non-homogeneous food during drying and to simultaneously solve them. A triply layered food of a slab shape consisting of starch and a mixture of starch and sugar, whose properties are well known and the moisture sorption characteristic is different with each other, was chosen [16]. Furthermore, an attempt to reduce and save the memory and CPU time for computer simulation of the model was performed [17]. The sensitivity of the analytical results on the drying behavior was discussed with comparing with those obtained by solving independently heat-moisture transfer and strain-stress of the layered foods, whose body was mesh-generated in different number of finite elements.

This paper is to introduce the outline of a series of the works performed in the past by the present author and his co-authors on drying-induced strain-stress and deformation of modeled media

2 Parametric analyses on effect of different heating modes

2.1 Modeling

Parametric analyses of the strain-stress combined with heat and moisture transfer in the drying process are performed. The transient three-dimensional problem of strain-stress as well as heat and moisture transfer in a slab of clay is solved simultaneously by the finite element method. Introducing the similar assumptions to Itaya *et al*. [5]to simplify the model, the governing equations of the heat and mass transfer are expressed in dimensionless form as:

$$\frac{\partial T^*}{\partial \theta} = -div(\mathbf{q}^*) + \dot{q}^*, \frac{\partial W^*}{\partial \theta} = -div(\mathbf{J}^*) \tag{1}$$

where

$$\mathbf{q}^* = -grad(T^*)\ ,\ \mathbf{J}^* = -\frac{1}{Le} grad(W^*) \tag{2}$$

The initial and boundary conditions are given by:

$$\theta=0\ ;\ T^*=0,\ W^*=1 \tag{3}$$

$$\theta>0\ ;\ Bi(1-T^*)+Bi_r(1-T^*)-BiN_h(H_e-H_a)=\mathbf{q}^*\cdot\mathbf{n} \tag{4}$$

$$BiLeN_m(H_e-H_a)=\mathbf{J}^*\cdot\mathbf{n} \tag{5}$$

In the equations, the dimensionless parameters are defined by:

$$\theta=Fo=t\alpha/l_0\ ,\quad T^*=(T-T_0)/(T_a-T_0)\ ,\quad W^*=W/W_0\ ,\quad X=x/l_0\ ,\quad Y=y/l_0\ ,$$
$$Z=z/l_0\ ,\quad Bi=hl_0/k\ ,\quad Le=\alpha/D_W\ ,\quad Bi_r=\sigma_r\varphi l_0(T_a^2+T_s^2)(T_a+T_s)/k\ ,$$
$$N_h=L_a/c_{pa}(T_a-T_s),\ N_m=c\rho V/c_{pa}\rho_0V_0W_0,\ \dot{q}^*=l_0^2\dot{q}/k(T_a-T_0) \tag{6}$$

where t is time, α and D_W are the apparent thermal and overall diffusion coefficients, T_a and T_s are temperatures of ambient and surface, respectively, W is moisture content, H_a and H_e are ambient humidity and equilibrium humidity at the surface temperature, c and c_{pa} are specific heat of clay and air, L_a is latent heat, V is the volume, σ_r and ϕ are Stefan-Boltzmann constant and blackness, $\dot{q}$ is the heat generation rate inside the body and the subscript 0 represents the initial condition. Introducing those parameters, we can discuss the effect of more general parameters on the drying behavior.

Similarly to the works by Itaya et al.[4, 5], approximating the free strain, that is the strain taking place under no internal stress defined by a function of only the local moisture content, the strain and stress are analyzed by a set of governing equations represented for viscoelastic media.

Constitutive equation:

$$\sigma_{ij}=\int_{t=0}^{t=\tau}G_{ijkl}\left(\xi(t)-\xi'(\tau)\right)\frac{f\varepsilon^*_{kl}\left(\xi(\tau)\right)}{f\tau}d\tau \tag{7}$$

where

$$G_{ijkl}(t)=\frac{1}{3}\left[G_1(t)-G_2(t)\right]\delta_{ij}\delta_{kl}+\frac{1}{2}G_1(t)\left[\delta_{ik}\delta_{jl}+\delta_{il}\delta_{jk}\right] \tag{8}$$

$$G_1(t)=2G(t)\ ,\ G_2(t)=3K(t) \tag{9}$$

$$\varepsilon^*_{ij}(t)=\varepsilon^*_{ij}(t)-\varepsilon^s_{ij}(t) \tag{10}$$

Equilibrium equation:

$$\sigma_{ij,j}+F_i=0 \tag{11}$$

Strain-displacement relation:

$$\varepsilon_{ij}=\frac{1}{2}\left(U_{i,j}+U_{j,i}\right) \tag{12}$$

where ξ and ξ' are the reduced times and equal t and τ, respectively. σ_{ij} and ε_{ij} are ij-th elements of the stress and strain tensor σ and ε, $\sigma_{ij,j}$ and $U_{i,j}$ denote differentiation of σ_{ij} and U_i with respect to j, G and K are shear and bulk moduli, F_i is body force, ε^*_{kl} and ε^s_{kl} are strain caused by the stress and shrinkage and δ is delta function. These equations are solved by the finite element method. The detail formulation appears in the papers by Itaya et al.[4, 5]

2.2 Analytical results and discussion

Intermittent heating is modeled so that a slab is heated alternatively with a high and low Biot number in every $\Delta\theta$ interval time. In the internal heating mode, the heat generation rate is given so that the sum of the convective, radiative and internal heating rates at $\theta = 0$ are equal to the rate in the hot air heating mode. Then the dimensionless heat generation rate is derived as

$$\dot{q}^* = 2\left(Bi + Bi_r\right)\left(\frac{1}{x_0} + \frac{1}{y_0} + \frac{1}{z_0}\right) l_0 \left(\frac{T_a^c - T_a}{T_a^c - T_0}\right) \tag{13}$$

where T_a^c denotes air temperature in the hot air heating mode. Referring Hasatani et al. [3], and Itaya et al. [4],Bi,1/Le and Bi_r are set a constant at 0.11, 0.2 and 0.15 respectively. In the intermittent heating mode, Bi is reduced stepwise to one-tenth at the low heating period. The internal heating is assumed to be operated under the temperature ratio, $(T_a^c - T_a)/(T_a^c - T_0)$= 5, in Eq.(13).

It is quite difficult to normalize the strain-stress equations, the saturated humidity and the shrinkage factor, relating to the heat and mass transfer since they are nonlinear with temperature and moisture content. Thus the same heat and moisture transfer properties as the past work [3] are employed for the conversion to dimensional parameters from the dimensionless ones. The initial temperatures of 293 K and the initial moisture content 0.249 kg-water/kg-dry solid are fixed for all runs. The air temperature is 343 K for the hot air and intermittent heating modes and 303 K for the internal heating mode. For the mechanical properties and the shrinkage factor, values given by the reference [3] are used, i.e. the bulk and shear moduli, $K(t)$ and $G(t)$ are determined from the following expressions.

$$K(t) = E(t) / 3(1\text{-}2\nu)\ ,\quad G(t) = E(t) / 2(1+\nu) \tag{14}$$

$$E(t) = 7.0\text{x}10^7 \exp(-\,t / 1.7\text{x}10^4)\ \ [\text{ Pa }]\ ,\quad \nu = 0.35 \tag{15}$$

The drying conditions are assumed to be symmetric with respect to X-axis. Hence the simulation is carried out for a quarter part of the slab. The initial size of the calculation domain is 1x1x0.4 (X_0 x Y_0 x Z_0) and the equivalence length l_0 is 0.03 m.

Figure **1** shows theoretical results on the profiles of moisture content and temperature in a several heating modes at a dimensionless time θ = 0.5. The profiles are drawn by contour curves on a half of the bisected face. As the air temperature only in the run of the internal heating mode is different from the other modes, the normalized temperature can not be compared at the same level with each other. Thus the temperature in the figure is modified so to adjust the same dimensionless temperature as one in the other heating modes. The dotted line is an original configuration of the slab before drying starts. In the intermittent heating mode, hot air heating by high and low Biot number, 0.2 and 0.02 is supposed to be repeated alternatively in every time interval of 0.1. While the gradient of the moisture content distribution seems to be larger than the other modes at θ= 0.5 in the high Biot number period, the gradient is significantly relaxed at the end of the low heating period as showing the profile at θ= 0.4 in Figure **2**. The temperature profile achieves almost uniform within the deviation of 0.01 at this time during continuous drying by the hot air heating mode. In the intermittent mode, the gradient of the temperature shows the opposite behavior to the moisture content if they are compared between the profiles in the low and high Biot number periods. This characteristic is explained by the effect of radiative heat transfer from the dryer wall, i.e. if the rate of convective heat transfer falls down, the contribution of radiative heat transfer appears significantly and the surface of a wet sample is heated so to rise toward a higher value than the wet-bulb temperature. In the internal heating mode, the temperature rises gradually inside the body and the gradient becomes significant as well since the heat sink region due to evaporation and/or convective heat loss lies on the surface exposed to the ambient.

The transient behavior of average moisture content and temperature in the slab, which is determined theoretically in a several modes, are shown in Figure **3**. The moisture content and temperature in the intermittent heating mode fluctuates above and under the results in the continuous convective heating mode, i.e. while the drying rate increases in the high heating period, temperature falls as described in the above section. Both the drying rate and

temperature rise significantly in the internal heating mode compared with the other modes although the heating rate given into the body is assumed to be equal to the other modes at the beginning of drying.The reason can be explained by the fact that the net heating rate falls gradually due to reduction of the temperature difference between hot air and the surface with elevation of the surface temperature in the convective heating while the internal heating is adopted with a constant rate through the drying period.

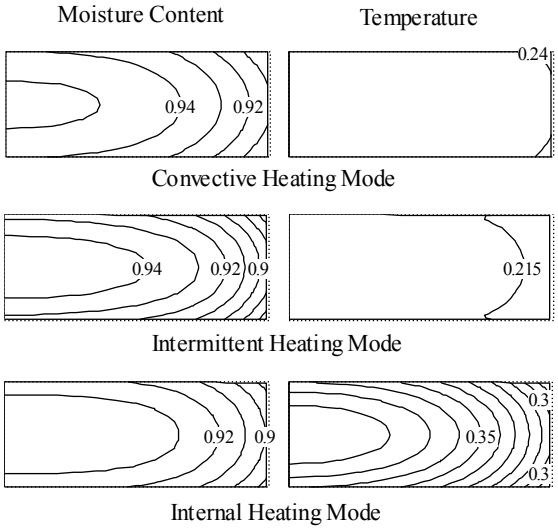

Fig. 1. Profiles of moisture content and temperature in different heating modes at θ= 0.5.

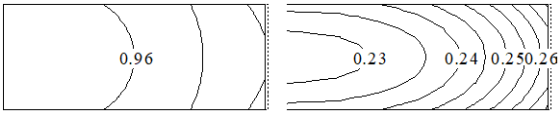

Fig. 2. Profiles of moisture content and temperature in the intermittent heating at θ= 0.4.

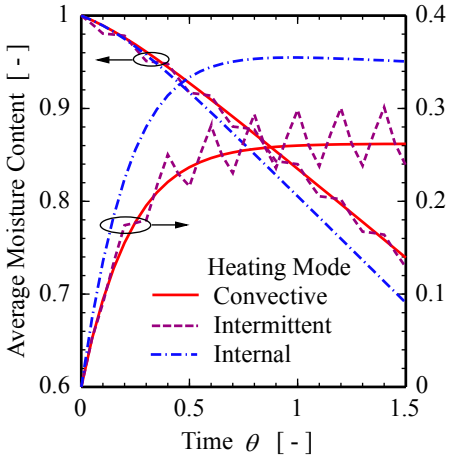

Fig. 3. Transient moisture content and temperature.

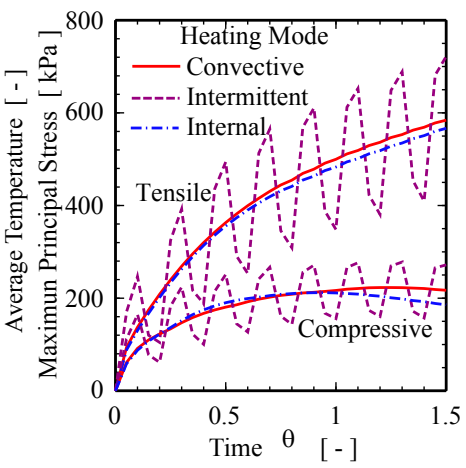

Fig. 4. Tensile stress against moisture content.

The time behavior of the maximum tensile and compressive stresses is compared among the heating modes in Figure **4**. Both the stresses oscillate and reduce appreciably during the

low Biot number period when the slab is heated intermittently. These behaviors can be predicted also from the average moisture content and temperature. In the internal heating mode, the maximum stresses are a slightly smaller than the convective heating particularly in the later period of drying. If tensile stress, which can be related with the cause of crack generation, is plotted against the moisture content, the effect of the internal heating on reduction of the stress is made clearer as drawn in Figure **5**. In general, as hot air drying proceeds rapidly at the corners of the slab where the temperature maintains the highest, the maximum stress appears around these portions. However, the drying rate is somewhat controlled there in the case of internal heating because the temperature becomes the lowest at the corners. This fact is considered as a reason of lower stress formation by internal heating than convective heating. Indeed the present analytical model takes account for no influence of temperature on the apparatus diffusivity of moisture in the slab. However, as vapor pressure increases exponentially with rising temperature, the moisture movement in the body will be enhanced by the internal pressure diffusion of vapor. This effect on the drying performance must be studied by further advanced model and experiment in the future. Intermittent heating contributes also a remarkable fall of the stress in the low heating period, but the stress results in loaded much strongly again in the high heating period. Hence it is implied that the internal heating mode may be the most effective one to drying of the slab if the drying-induced stress is compared among those heating modes under a limited simulation in the present work.

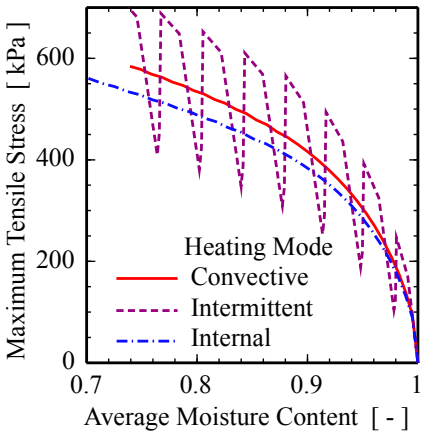

Fig. 5. Tensile stress against moisture content.

3 Drying experiments by microwave heating

Drying experiments of ceramics molded into a slab are conducted by applying microwave to examine the effect of the internal heating on drying characteristic and crack generation behavior. Figure **6** shows an outline of the applicator in the experimental setup. The applicator is made of a steel duct with 100 x 100 mm in cross section and 500 mm in length. The test section is located in the center of the duct, and a plate of ϕ50 mm of diameter for a sample holder is connected to an electronic balance to measure the time behavior of sample weight during drying. A window with a door of steel plate is placed at the side of the test section for putting the sample in and out. Microwave generated in a magnetron (Tokyo Electronics Inc., IMG-2501S) was transmitted to the sample through the waveguide joint on the test section from the above. The frequency is 2,450 MHz and the power varies from 100 to 1,000 W. An isolator, a stab-tuner and a power monitor are installed for tuning microwave between the magnetron and the applicator. Convective heating can take place simultaneously

by flowing hot air in the duct of the applicator. Steel wire nets are set at both the inlet and outlet of the test section in the duct to seal the microwave from leaking out. The open face on the duct joint with the waveguide is covered by a glass plate to prevent the turbulence of hot air flowing in the duct and diffusion of steam evaporated into the waveguide.

Drying by convective heating was performed without irradiation of microwave using the same dryer as in Fig. 6. The drying behavior by microwave heating and convective heating are compared with the data by radiation heating in an oven type dryer (Yamato, Drying Oven DX31).The samples were prepared by molding kaolin into a slab as following: the dry powder of kaolin 50 g mixed with 20 g water was pressed in the mold made of aluminum with the pressure 200 kPa. The slab size was 60x60x10 mm. The kaolin is used industrially for tile production with the median particle size, 0.75 μm. The sample was put horizontally keeping out a clearance with small spacer on the holder in the test section so that a surface of the slab faced to incident microwave and the both sides were subjected to parallel flow of air. The drying rate was determined from the time behavior of the sample weight measured by electronic balance. The transient temperatures were measured by luminescence types of optical fiber thermometer (Anritsu Instrument, FX-8500) placed at the center core and the surface of the sample.

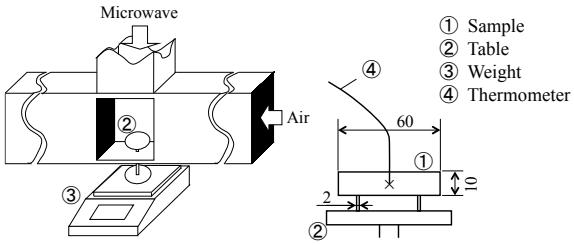

Fig. 6. Outline of applicator for microwave drying experiment.

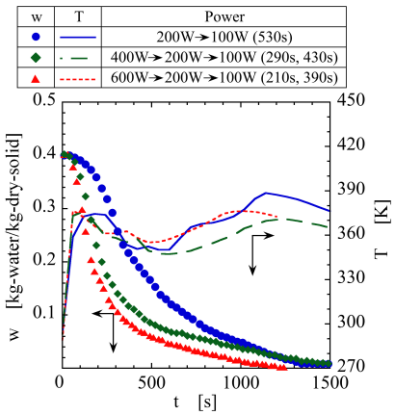

Fig. 7. Transient behavior of kaolin slab by microwave heating controlled dynamically.

It was implied that a rise in the internal temperature up to the boiling temperature of water causes crack by the expansion throughthe experiments. In order to complete microwave drying of molded samples without crack generation in as short time as possible, a control of the internal temperature must be a key factor. Here, microwave power was controlled dynamically in the progress of drying. The time behaviors of the moisture content and the internal temperature were plotted in Figure **7** when the experiments were performed in three dynamic patterns of the power: the first one is 200 W for the first 530 seconds and sequentially maintaining 100 W until the drying completion, the second one 400 W for the

first 290 seconds, 200 W for the next 430 seconds and 100 W, and the last one 600 W for the first 210 seconds, 200 W for the next 390 seconds and 100 W. The internal temperature was maintained under the boiling point except in the last period of drying for any dynamic control pattern. Crack generation was not observed on the sample through the drying period as well. The drying time was reduced remarkably until approximate 1,500 seconds and less while it was the order of 10^4 seconds in the oven dryer and over 4,000 seconds in hot air drying. Particularly the third pattern was only 1,250 seconds. From these facts, it is found that dynamic microwave heating contributes greatly to drying enhancement of molded ceramics.

4 Drying of triply layered nonhomogeneous foods

4.1 Modeling

Governing equations for the transient heat and moisture transfer in food are expressed by modifying the conservation equations [15] on the phase change of moisture as follows, respectively:

$$c_p\rho_b\frac{fT}{ft} = -\mathrm{div}(\mathbf{J_h}) + \sum_j \Delta H_r R_j + \Delta H_v \varepsilon \frac{fC}{ft} \tag{16}$$

$$\frac{fC}{ft} = -\mathrm{div}(\mathbf{J_m}) + \square_j R_j + \varepsilon\frac{fC}{ft} \tag{17}$$

where C is moisture concentration given by the unit kg-moisture/m^3-wet solid, ΔH is enthalpy, R reaction rate, T temperature, t time, ε is the parameter on the rate of internal moisture vaporization or condensation. Assuming the fluxes due to heat conduction and moisture transfer for heat transfer and due to the gradients of moisture concentration, temperature and pressure for moisture transfer, the total fluxes, $\mathbf{J_h}$ and $\mathbf{J_m}$ in Eqs.(16) and (17) are expressed as

$$\mathbf{J_h} = -\mathbf{k_t}\times\mathrm{grad}(T) - (-1)^m\mathbf{k_c}\times\mathrm{grad}(C) - (-1)^n\mathbf{k_p}\times\mathrm{grad}(P) \tag{18}$$

$$\mathbf{J_m} = -\mathbf{D_w}\times\mathrm{grad}(C) - \mathbf{D_t}\times\mathrm{grad}(T) - \mathbf{D_p}\times\mathrm{grad}(P) \tag{19}$$

where $\mathbf{k_t}$, $\mathbf{k_c}$ and $\mathbf{k_p}$ are the thermal conductivity, the Dufour thermal conductivity and the filtrational thermal conductivity, respectively and $\mathbf{D_w}$, $\mathbf{D_t}$ and $\mathbf{D_p}$ are the mass diffusivity, the Soret mass diffusivity and the pressure mass diffusivity, respectively. To apply the governing equations to the moisture transfer in non-homogeneous food, whose components have generally different moisture sorption characteristics with each other, the concept of the mass transfer potential ϕ [15] defined by following equation was introduced

$$dW = \left(\frac{fW}{f\phi}\right)_T d\phi + \left(\frac{fW}{fT}\right)_\phi dT \tag{20}$$

where W represents the moisture content and is related easily to the water concentration. Substituting Eq. (20) into Eqs. (16) and (17), the equations are rewritten as:

$$\left\{c_p\rho_b - \Delta H_v\varepsilon\left(\rho_s + \frac{f\rho_s}{fW}W\right)C_T\right\}\frac{fT}{ft} - \Delta H_v\varepsilon\left(\rho_s + \frac{f\rho_s}{fW}W\right)C_m\frac{f\phi}{ft} = -\mathrm{div}(\mathbf{J_h}) + \sum_j \Delta H_r R_j \tag{21}$$

$$\left(\rho_s + \frac{f\rho_s}{fW}W\right)\left(C_m\frac{f\phi}{ft} + C_T\frac{fT}{ft}\right) = -\mathrm{div}(\mathbf{J_m}) + \sum_j R_j \tag{22}$$

$$C_T = \left(\frac{fW}{fT}\right)_\phi, C_m = \left(\frac{fW}{f\phi}\right)_T \tag{23}$$

The mass transfer potential can be substituted by the potential corresponding to Gibbs free energy in a wet materials. Then the mass transfer potential is determined by (Luikov, 1975)

$$\phi = \mu_0(T) + RT\ln(a_w) \tag{24}$$

where a_w is an activity and is related to W by GAB equation form (Lomauro et al., 1985) or an isotherm curve of food.

$$W = \frac{w_m C K_a a_w}{(1-K_a a_w)(1-K_a a_w + C K_a a_w)} \tag{25}$$

where K_a is a constant. μ_0 is the chemical potential in the state of pure saturated water.

$$\mu_0 = \Delta G^0 = \Delta H^0 - T\Delta S^0 \tag{26}$$

ΔG^0 and ΔS^0 are the Gibbs free energy and the entropy, respectively.

A linear viscoelasticity, that is suggested as a reliable behavior of strain-stress for several foods, was assumed. The governing equations for a viscoelastic boundary value problem are represented as the same formulas in Eqs. (7) to (12). Here the reduced time, ξ and ξ' in Eq. (7) are defined to modify temperature and moisture content dependency on stress by extending or reducing the effective time as

$$\xi = \frac{t}{a_T(T)a_M(W)}, \quad \xi' = \frac{\tau}{a_T(T)a_M(W)} \tag{26}$$

where a_T and a_M are temperature and moisture shift factors, respectively.

Additionally the equilibrium equation and the strain displacement relation are necessary, but they are the same as conventional ones [16].

4.2 Sample preparation

The hydrates of two different components were used as a representatively nonhomogeneous food sample: 1) Hylon VII starch (63.2% amylose starch provided by the National Starch and Chemicals Co.), 2) mixture of Hylon VII (75%) and sucrose (25%). The former one abbreviated by H while the latter one by S later. Each component was layered as seen in Figure **8**. The moisture sorption characteristics of two components are shown in Figure **9**.

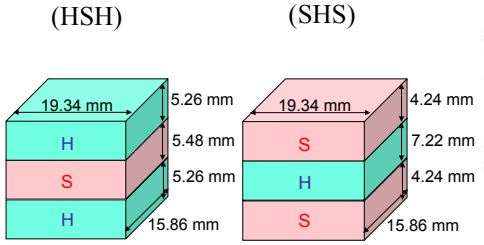

Fig. 8. Nonhomogeneous food sample layered.

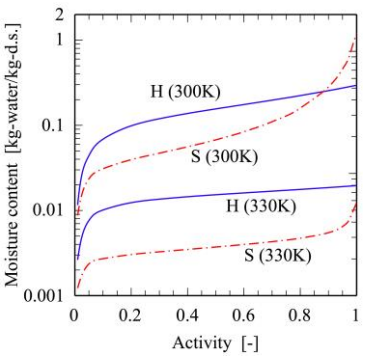

Fig. 9. Sorption isotherm of components H and S.

4.3 Drying behavior and internal stress formation

Figure 10 and 11 compare the experimental data on the temperature and moisture content of the triply layered sample subjected to drying with theoretical results obtained from the present analytical method. In the figures, W_1, W_2 and W_{av} are average moisture content in the outside, the inside and the whole layers, respectively. The contents are normalized by the initial moisture content. The physical properties of the sample required for the simulation are referred from the literature [14]. A large difference of time behavior of average moisture content was observed between HSH and SHS due to the difference of sorption isotherm between H and S. The moisture content in the outside layers for SHS is remarkably reduced with the drying time and is lower than that in the inside layer through whole drying time. The moisture content in the outside layers for HSH is much close to that in the inside layer. "Calc. 1" and "Calc. 2" correspond to the results solved numerically by using meshes divided into 150 and 1200 elements, respectively. The numerical result solved with 1200 elements agrees better with the experimental results than that with 150 elements for both the HSH and SHS, and a little deviation was observed between Calc. 1 and Calc. 2.

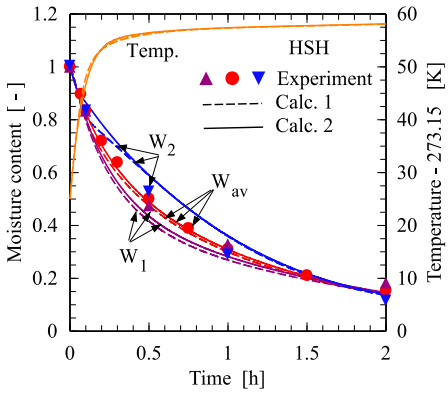

Fig. 10. Transient moisture content of each layer and temperature in the core center (HSH).

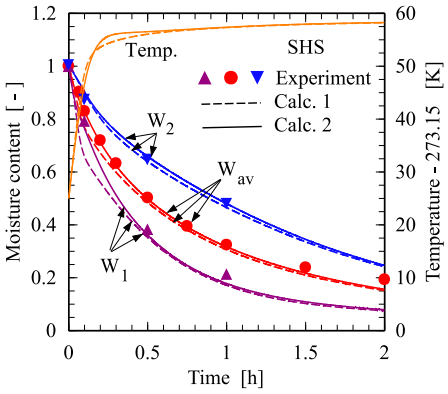

Fig. 11. Transient moisture content of each layer and temperature in the core center (SHS).

Figure 12 shows the maximum principal stress analyzed by the theoretical model against the drying time. The maximum magnitude of tensile and compressive stresses generated inside the body is plotted to compare the analytical accuracy between Calc. 1 and Calc. 2. It is considered that a crack may be formed by tensional stress of a critical magnitude. In the beginning of drying of 0.1 to 0.2 hour, a peak of tensile and compressive stresses was observed in the sample. The location was identified in the area of exposed surface for tension and the zone close to the interface of two components for compression from the stress distribution.

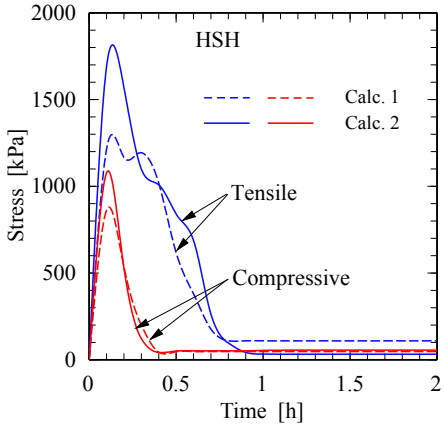

Fig. 12. Transient maximum tensile and compressive stresses in HSH.

Figure 13 shows examples of moisture content and temperature profilespredicted analytically at 1.0 hour of drying for HSH. The profiles compare the solution obtained from the combined analysis of heat and moisture transfer and strain-stress with strain-stress free analysis. The contours indicate the distribution on one-fourth of the bisected face of the samples because of its symmetric shape. Thus the point of $x = y = 0$ corresponds to a core center of the sample. The horizontal line in the body is an interface of two components. The temperature distributions are fairly uniform at this short drying time. The discontinuity of moisture content appeared on the interface. The moisture content in the inside layer close to the interface is lower than that of the outside layer for the sample of HSH. The reason is due to the fact that the mass transfer potential of S is greater than H at this moisture levels around the interface. This fact means that the moisture content of H becomes higher than S when the mass transfer potential or activity is same.On the other hand, both the analyses of heat-moisture transfer with and without strain stress give the almost same profiles of moisture content and temperature. From these analyses, the profiles of moisture content and temperature predicted will be less sensitive to strain-stress formation as far as weak drying-induced shrinkage takes place in a similar level to the present samples at least (<1%). This fact suggests that the drying behaviors can be analyzed accurately with short CPU time unless strain-stress equations are solved simultaneously.

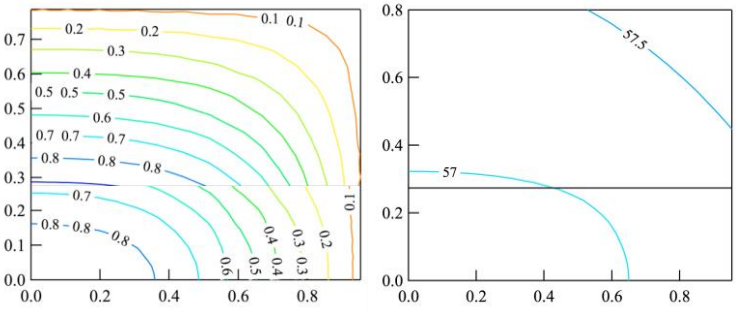

(a) Moisture content (strain-stress) (b) Temperature (strain-stress)

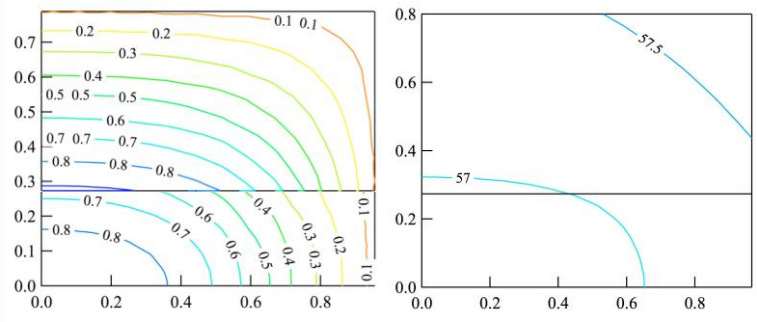

(c) Moisture content (strain-stress free) (d) Temperature (strain-stress free)

Fig. 13. Profiles of moisture content and temperature in HSH at drying time 1.0 h (1200 elements).

5 Conclusions

The outline of a series of the works was introduced on drying-induced strain-stress and deformation of modeled media performed by the present author and his co-authors. They are summarized as:

1. The transient three-dimensional problem of strain-stress and heat and moisture transfer was solved simultaneously by the finite element method.
2. The behaviors of internal strain-stress formation and deformation are compared among three modes of hot air heating, intermittent heating and internal heating for a ceramic slab.
3. The internal heating modemaintains stress formation at the lowest level and can enhance drying rate in the three modes.This effectiveness of the internal heating is examined by employing the microwave heating. Microwave heating enhanced significantly drying rate without crack formation compared with convective heating.
4. Drying of three layered foods consisting of two ingredients wasmodeled introducing the concepts of the mass transfer potential and a linear viscoelasticity to consider the different sorption isotherm and creep phenomenon.
5. The combination of different foods influences significantly not only the drying characteristic but also the internal strain-stress generation.
6. The drying behavior could be analyzed with a high accuracy even if only heat and moisture transfer were solved without strain-stress analysis.

References

1. I. Shishido, T. Maruyama, M. Funaki, S. Ohtani, Kagaku KogakuRonbunshu, **13**(1), 78 (1987)
2. I. Shishido, T. Muramatsu, S. Ohtani, Kagaku KogakuRonbunshu, **14**(1), 87 (1988)
3. M.Hasatani, Y. Itaya, K. Hayakawa, Drying Technology, **10**(4), 1013 (1992)
4. Y.Itaya, S. Mabuchi, M. Hasatani, Drying Technology, **13**(3), 801 (1995)
5. Y. Itaya, S. Taniguchi, M. Hasatani, Drying Technology, **15**(1), 1 (1997)
6. Z. X. Gong, A. S. Mujumdar, Y. Itaya, S. Mori, M. Hasatani, Drying Technology, **16**(6), 1119 (1998)
7. Y. Itaya, K. Okouchi, S. Mori, Drying Technology, **19**(7), 1491 (2001)
8. Y. Itaya, S. Uchiyama, S. Hatano, S. Mori, Drying Technology, **23**(6), 1243 (2005)
9. Y. Itaya, S. Uchiyama, S. Mori, Transport in Porous Media, **66**(1-2), 29 (2007)

10. R. J. Gustafson, D. R. Thompson, S. Sokhansany, Trans. ASAE, **22**, 955 (1979)
11. R.N. Misra, J.H. Young, Trans. ASAE, **24**(3), 751 (1981)
12. K. Haghighi, L.J. Segerlind, Trans. ASAE, **31**(3), 930 (1988)
13. K. Haghighi, L.J. Segerlind, Trans. ASAE, **31**(3), 938 (1988)
14. T.Tsukada, N. Sakai, K. Hayakawa, J. Food Sci., **56**(5), 1438 (1991)
15. A.V.Luikov, Int. J. Heat Mass Trans., **18**(1), 1 (1975)
16. Y. Itaya, T. Kobayashi, K. Hayakawa, Int. J. Heat and Mass Transfer, **38**(7), 1173 (1995)
17. Y. Itaya, N. Kobayashi, Proc. 17th International Drying Symposium (IDS 2010), Magdeburg, Germany, 3-6 October (2010)